UPDATE ON Nb$_3$Sn PROGRESS AT CORNELL UNIVERSITY*

R. D. Porter[†], T. Arias, P. Cueva, J. Ding, D. L. Hall, M. Liepe, D. A. Muller, N. Sitaraman
Cornell Laboratory for Accelerator-Based Sciences and Education (CLASSE)
Ithaca, NY 14853, USA

Abstract

Niobium-3 Tin (Nb$_3$Sn) is the most promising alternative material for SRF accelerator cavities. The material can achieve higher quality factors, higher temperature operation and potentially higher accelerating gradients compared to conventional niobium. Cornell University has a leading program to produce 2 - 3 micrometer thick coatings of Nb$_3$Sn on Nb for SRF applications using vapor diffusion. This program has been the first to produce quality factors higher than achievable with conventional Nb at usable accelerating gradients. Here we present an update on progress at Cornell University, including studies of the formation of the Nb$_3$Sn layer, density functional theory calculations of Nb$_3$Sn growth, and designs for a sample host cavity for measuring the quench field of Nb$_3$Sn.

INTRODUCTION

Nb$_3$Sn is a promising alternative material for SRF accelerator cavities due to a T_c of 18 K and a superheating field of $\approx$ 400 mT [1]. This allows for higher quality factors, higher temperature operation, and for accelerating gradients twice that of conventional niobium. Cornell University has a program for creating Nb$_3$Sn cavities using vapor deposition of tin onto a niobium cavity to form a 2 - 3 µm Nb$_3$Sn layer [1–5]. Current Nb$_3$Sn cavities produced at Cornell achieve Q $\approx 10^{10}$ at 4.2 K and $\approx$ 16 MV/m in continuous wave operation [6].

The superheating field of niobium suggests that the maximum achievable accelerating gradient for a 1.3 GHz TESLA style cavity should be $\approx$ 90 MV/m, far higher than what is currently achieved. Klystron pulsed test measurements and T-mapping show that the maximum gradient is being limited by thermal quench at a defect [7]. Two main candidates have been suggested: flux vortex entry at particularly vulnerable grain boundaries [8]; and areas of tin depleted Nb$_3$Sn where the atomic percentage of tin is lower, causing the superheating field to be suppressed [7].

The tin depleted sites can appear both on the surface of the Nb$_3$Sn and within the layer (see Fig. 1). The surface depletions sites are likely formed late in the coating process after all free tin has been used and tin starts being pulled from the surface to form Nb$_3$Sn at the Nb-Nb$_3$Sn inferface. The tin depletion defects within the Nb$_3$Sn are often deep enough to be shielded from the RF, but any chemical polishing to

reduce surface roughness or remove surface defects could expose the tin depleted sites. For this reason, it is critical to deal with the tin depleted defects both on the surface and in the bulk.
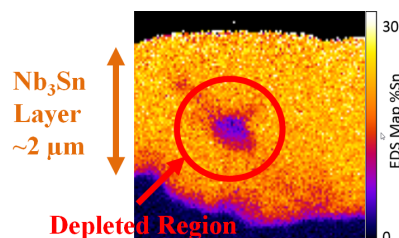

Figure 1: An EDS cross-section of a Nb$_3$Sn layer showing a tin depleted region within the Nb$_3$Sn layer.

Here we present an update on progress at Cornell University towards increasing the maximum accelerating gradient. This paper primarily concerns itself with studying how the Nb$_3$Sn layer forms through both experimental and theoretical methods, so that coating methods can be changed to suppress the formation of defects. A brief update is included on the development of a high field sample host cavity to measure the quench field of Nb$_3$Sn and other materials.

Nb$_3$Sn GROWTH PROCESS

The most successful method to create SRF suitable Nb$_3$Sn is vapor deposition of tin onto niobium, in which a niobium cavity is placed in a high temperature vacuum furnace and then tin is vaporized at a high temperature and allowed to absorb into the niobium [4]. This is done at a temperature > 1000 °C where, in a tin rich environment, only Nb$_3$Sn and liquid tin may form. SnCl$_2$ is used to nucleate tin onto the surface of the cavity. Cornell uses a secondary heater to heat the tin source to increase the vapor pressure of tin separate from the Nb$_3$Sn growth rate, allowing the availability of tin to be controlled and increase the availability of tin while the temperature is ramping up. A typical coating temperature profile is shown in Fig. 2.

LAYER GROWTH STUDIES

In order to understand how defects on the surface form, and in order to find ways of altering the coating process to remove defects we are examining how the Nb$_3$Sn layer forms. This is done by placing niobium samples in our coating furnace and stopping the coating at various temperatures while the temperature is increasing from the nucleation temperature to the coating temperature; a process we believe is critical to the formation of a good Nb$_3$Sn layer.
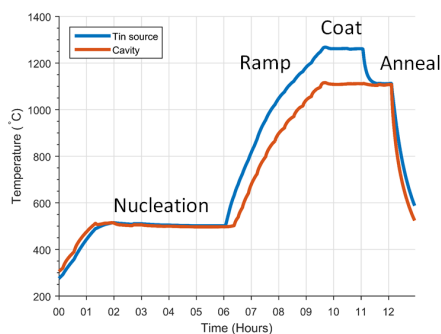
Figure 2: Temperature during Nb_3Sn coating showing both the cavity and the tin source temperatures. Not shown is a 24 hr degas period at 180 C prior to nucleation.

Figure 3 growth shows false colored SEM images of the surface of these samples for two different surface preparations before coating: a normal BCP niobium surface, and a BCP niobium surface that has been anodized to form a ≈ 70 nm oxide, which has been previous shown remove certain surface defect and decrease the surface resistance [6]. These samples were coated in pairs, ensuring that the cutoff temperatures were identical.

As the layer grows, for both sets of samples, we can first see tin on the surface, then see structures start to form on the surface. At certain temperature these structures break down into multiple grains: likely an indication that another Nb-Sn compound has formed, and then underwent a phase transition at a critical temperature. Eventually a thin Nb_3Sn layer has formed.

Interestingly, anodization significantly changes the surface morphology of the samples. The anodized samples appear to have more tin (red and purple in nucleation images) on the surface after nucleation. The crystal structures on the surface are much larger on the anodized samples. This could be indicative of more tin gathering on the surface before the Nb_3Sn starts to form by the oxide either: acting as a barrier that must be destroyed before Nb_3Sn can form, or by somehow encouraging the depositing on tin early in the process. In the end the unanodized surface forms a large, thin crystal grain (highlighted in green), which is too thin to fully shield the RF, resulting in increased losses.

GROWTH DYNAMICS

Density Functional Theory calculations have improved our understanding of how tin-depleted regions form in Nb_3Sn. We model the phase as an A15 crystal in which niobium substitutional defects can occupy tin lattice sites, thus allowing for tin depletion. Using the cluster expansion method with Monte Carlo sampling, we can calculate the equilibrium concentration of these defects, and therefore the equilibrium stoichiometry of the phase, as a function of temperature and tin chemical potential.

This calculation accurately reproduces the experimentally observed stoichiometry range and indicates that the tin depletion defects should tend to spread evenly throughout the
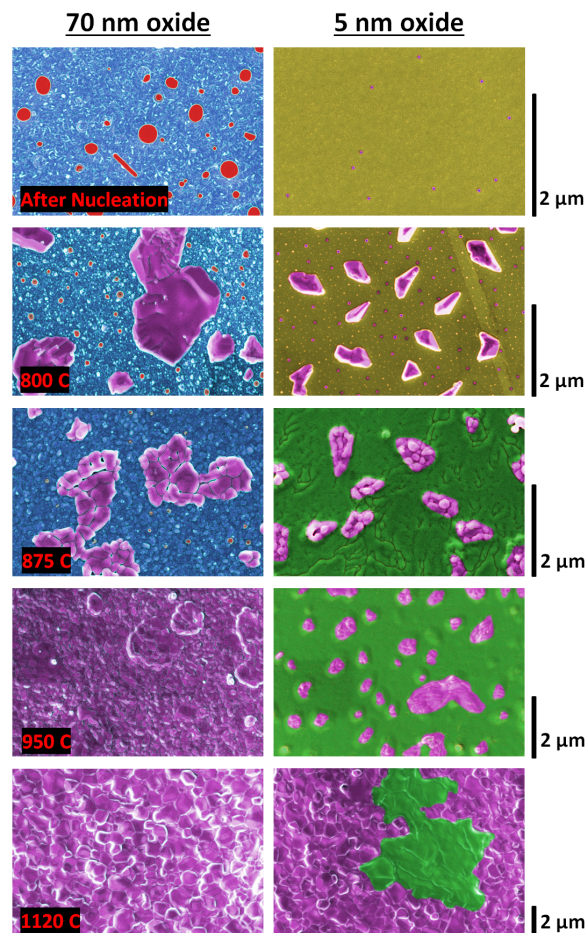

Figure 3: False colored SEM images of samples being coating in Nb_3Sn that were terminated during the temperature ramp up from nucleation to coating steps (see Fig. 2). Two different preparations are shown: one in which a sample was anodized to grow a 70 nm oxide and one with the natural oxide layer. The images have been false colored to highlight regions with different morphology. Original SEM images (not false colored) published in [6].

crystal due to repulsive pairwise interactions, not cluster at any preferred density as observed. This suggests that the tin depleted regions we observe in our layers are likely a result of kinetic processes, in particular varying tin chemical potential during layer growth, rather than phase separation.

Based on this result, we plan to alter our coating procedure to ensure a steady supply of liquid tin to the growing layer, thereby maintaining the tin chemical potential at a level conducive to tin-rich Nb_3Sn growth (see Fig. 4). We hope to verify that doing so indeed prevents the formation of tin-depleted regions in Nb_3Sn.

HIGH FIELD SAMPLE HOST CAVITY

Advancing the accelerating gradient will require testing multiple coating processes to find the correct recipe and give feedback to growth models. For this reason, we are creating a sample host cavity to measure the quench fields of our
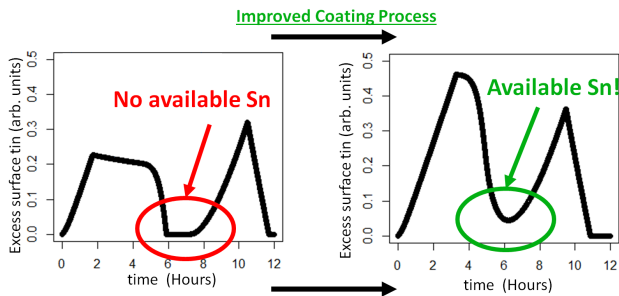
Figure 4: Hypothetical availability of tin during the coating process starting at the beginning of the nucleation step. Left: in the current coating process excess tin is being exhausted during the temperature ramp causing tin depleted region to form at that time (within the final Nb_3Sn layer). Right: With more tin added during this phase (by, say, increasing the amount of $SnCl_2$) excess tin is not exhausted during the ramp.

samples. This cavity is being designed to obtain high surface magnetic fields on the sample. We have decided upon using copper host cavity and using klystron high pulsed power. Due to the low quality factors endemic to copper cavities we must then use thermometry to detect quench.

Previous [9, 10] work has shown designs for a sample host cavity with a shape optimized to increase peak fields on the sample (at expense of field uniformity) and an elliptical sample shape to further amplify the peak magnetic fields on the sample (see Fig. 5). The cavity operates in a TE-111 mode at 1.3 GHz (compatible with Cornell's R&D klystron). The peak fields on the sample reach can reach > 400 mT for 1 J in the cavity.
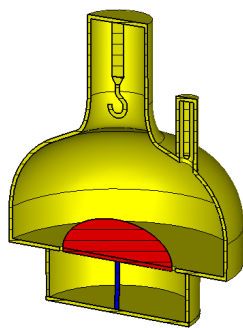

Figure 5: A design cross-section of the high field sample host cavity. The host cavity is in yellow, the sample is in red, and the sapphire support rod is in blue.

Coupler designs have now been developed (see Fig. 5). The field distribution requires the use of a loop coupler (magnetic coupling). The distance of the coupler is adjustable on an already existing test stand/insert. With the range of this test stand the coupling factor, β, can be adjusted from $\beta < 1$ to $\beta = 150$.

With 100 kW of forward power the peak field can reach 400 mT in 14 μs (see Fig. 6). This rise time is much faster than we can achieve in single cell cavities. This carries an

added bonus that it will allow us to probe further into the thermal runaway, allowing for us to better experimentally determine the superheating field in quench field vs temperature tests [7]. A transmitted power coupler has also been added and has negligible impact on the field distribution.
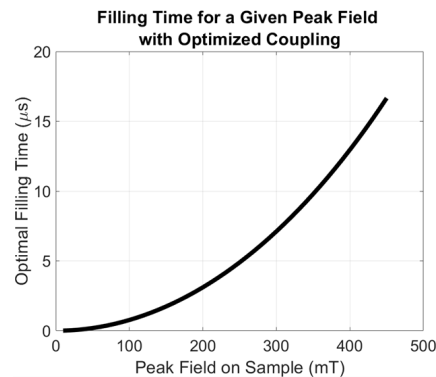

Figure 6: The filling time to given field with coupling optimized for that field. In this plot β reaches a maximum of 150.

Due to the host cavity being made from copper, the sample must be thermally isolated from the host. This is accomplished by creating a gap between the sample and the host. This requires the addition of a second chamber and supporting the sample on a rod. Previous work showed that the use of a sapphire support rod is needed to reduce the field in the bottom cavity [10]. Thermal simulations show that the thermal transport through the sapphire rod is sufficient to prevent thermal runaway on the time scale of the pulse lengths, and the pulse repetition rate is slow enough to allow for the sample to return to the bath temperature between pulses.

CONCLUSION

The layer growth studies demonstrate the complexities of the forming Nb_3Sn layer and show a promising first step to understanding how the layer forms and is changed by different coating recipes. These layer growth studies will be used to inform the development of growth models. Surface analysis is currently underway to determine the compounds that are present on the surface during the layer formation. Density functional theory calculations are providing great insight into the formation of the Nb_3Sn layer. Current results suggest we could eliminate tin depleted defects within the Nb_3Sn layer.

The development of a sample host cavity for testing quench fields will lead to a useful tool in advancing the accelerating gradient. The electromagnetic, structural and thermal simulations of this cavity are complete, but a few final design considerations must be completed. Soon design schematics will be made and construction will commence.

REFERENCES

[1] S. Posen and D. L. Hall, "Nb3Sn Supercondcution Radiofrequency Cavities: Fabrication, Results, Properties, and

Prospects," *Superconductor Science and Technology*, vol. 30, no. 3, p. 33004, 2017.

[2] D. L. Hall, J. J. Kaufman, M. Liepe, R. D. Porter, and J. Sears, "First Results From New Single-Cell Nb3Sn Cavities Coated at Cornell University," in *Proc. of IPAC 2017*, Copenhagen, 2017.

[3] D. L. Hall, M. Liepe, and J. Maniscalco, "RF Measurements on High Performance Nb3Sn Cavities," in *Proc. of IPAC 2016*, Busan, May 2017.

[4] S. Posen, "Understanding and Overcoming Limitation Mechanisms in Nb3Sn Superconducting RF Cavities," Ph.D. dissertation, Cornell University, 2014.

[5] D. L. Hall, "New Insights into the Limitations on the Efficiency and Achievable Gradients in Nb3Sn SRF Cavities," Ph.D. dissertation, Cornell University, 2017.

[6] D. L. Hall *et. al.*, "High Performance Nb3Sn Cavities," in *Proc. of SRF 2017*, Lanzhou, China, July 2017.

[7] D. L. Hall, J. J. Kaufman, M. Liepe, J. T. Maniscalvo, and R. Porter, "High Performance Next-Generation Nb3Sn Cavities for Future High Efficiency SRF LINACs," in *Proc. of LINAC 2016*, East Lansing, Michigan, Sept 2016.

[8] D. L. Hall *et. al.*, "Cavity Quench Studies in Nb3Sn using Temperature Mapping and surface Analysis of Cavity Cut-Outs," in *Proc. of SRF 2017*, Lanzhou, China, July 2017.

[9] R. Porter, M. Liepe, J. T. Maniscalco, and V. Veshcherevich, "Sample Host Cavity for Measuring Flux Entry and Quench," in *Proc. of IPAC 2017*, Copenhagen, 2017.

[10] R. Porter, M. Liepe, J. T. Maniscalco, and R. Strauss, "Update on Sample Host Cavity Design Work for Measuring Flux Entry and Quench Field," in *Proc. of SRF 2017*, Lanzhou, China, July 2017.